NAVIGATION: *Journal of The Institute of Navigation*
Vol. 23, No. 1, Spring 1976
Printed in U.S.A.

Time Reference Microwave Landing System Multipath Control Techniques

R. J. KELLY

Abstract

THE TIME REFERENCE SCANNING BEAM (TRSB) landing system is an air-derived data system which operates at microwave frequencies to provide guidance information proportional to an aircraft's lateral and vertical displacement from a selected flight profile. Angular position of an aircraft is measured in the aircraft by receiving ground generated fan beams which scan "to" and "fro" across the coverage sector in both azimuth and elevation. The airborne subsystem measures the elapsed time between a given "to"-"fro" scan. The time difference is controlled to be an indication of the aircraft's angular position. This indicated angle could be corrupted by multipath. Basic to the TRSB concept is the azimuth and elevation controlled antenna radiation patterns (both in the scan and non-scan dimensions) which, in conjunction with their high scan rates, control the multipath to an operationally acceptable level. Since the multipath is controlled primarily on the ground, there is no special impact on the cost of the airborne equipment because simple, conventional RF and signal processing techniques need only be implemented into the airborne receiver hardware.

Introduction

This paper presents an exposition of the multipath control techniques used in the Microwave Landing System (MLS) which is presently under development by the U.S. Department of Transportation's Federal Aviation Administration (FAA) under the joint sponsorship of the FAA, NASA and DOD. The system is in conformance with requirements established by the All Weather Operations Panel of the International Civil Aviation Organization (ICAO). It satisfies the international need for a new nonvisual approach and landing system by utilizing a TRSB technique which has evolved from more than fifteen years of development effort on scanning beam systems in the U.S.

The TRSB is an air-derived system in which position is measured directly in the aircraft, rather than relying on the relay of ground-derived data from ground to air.

The objective of the US MLS program is to provide a common civil/military system which is capable of a wide range of both airborne and ground equipment configurations and satisfies the operational requirements and economic considerations of each category of user. This includes simple equipment for general aviation, more sophisticated systems for all-weather automatic landings, and transportable systems for specialized military applications. However, all airborne and ground based components will be fully compatible or "interoperable" with each other.

To successfully meet these objectives the TRSB must combat multipath signals which are introduced by unwanted reflections from obstacles in the airport environment. The MLS multipath literature is extensive and any attempt to summarize the analytical and experimental results to date would be a major undertaking. The intent of this paper is not to extend the studies performed to date but rather to firmly establish the fundamental multipath induced error mechanism

The author is with The Bendix Corporation, Communications Division, Baltimore, MD 21204. *He presented this paper at The Institute's 31st Annual Meeting in Washington, DC on June 24, 1975.*

so that the general reader may more readily understand and evaluate the principles behind many of the techniques proposed for its control. The computer simulation studies described in this paper were performed by Bendix during its recent MLS Phase II Feasibility Program.

Primary multipath effects and related phenomena treated in this paper are in-beam and out-of-beam multipath, and techniques for controlling the effect of these multipath signals is the subject of this paper. Its thrust is that multipath effects can best be eliminated in an operational sense by employing controlled ground antenna radiation patterns. In this way undesired radiation impinging upon airport obstacles and terrain is restricted at its source.

Multipath control is the principle feature which allows for low site preparation cost for future airports and the economical implementation of MLS at existing airports. Multipath control is quantified in this paper through the use of a simple equation which dictates the way the system parameters may be varied to achieve cost-effective performance. The landing system described below will meet or exceed the ICAO All-Weather Operational Requirements.

Brief Description of the TRSB Technique

The TRSB is an air-derived system which indicates a point in space by making two angle measurements and a range measurement. The angle measurements are based upon the detection of a narrow fan beam sweeping past an aircraft while the range measurement uses DME. The DME is an independent function and will be treated separately from the angle measurements. The ICAO MLS operational requirements specify that the signal-in-space should be generated over a wide angle coverage volume. This requirement is met by sweeping the service volume with narrow scanning fan beams and thereby generating a continuum of approach paths.

The scanning beam can be viewed as the sampling element in a sampled data system wherein the approach paths are reconstructed from the data samples. That is, the aircraft position is calculated at discrete time intervals as shown in Fig. 1. The airborne subsystem functions to obtain precision azimuth and elevation data suitable for display to the pilot or for automatic inputs to the aircraft's flight control system.

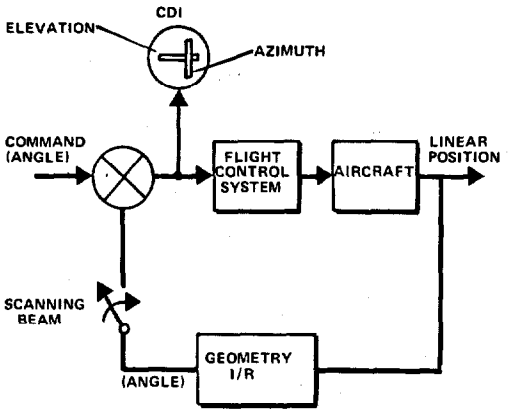

Fig. 1—The Landing System Block Diagram.

The TRSB is self-encoding and requires no form of modulation (Fig. 2). In addition other information, such as angle guidance function identification, facility identification and performance category is transmitted independently throughout the coverage volume on a broad sector pulse beam (Fig. 3). This broad sector transmission precedes each scanning beam transmission and is called the "preamble". Its modulation is direct differential phase shift keying (DPSK) of the RF carrier.

The output data samples, one for each pair of beam scans, can be reconstructed to an analogue signal by a simple zero order hold circuit or they can be inputed directly to flight control systems (FCS) which employ digital autopilots.

The principle premise of MLS is the specification of a universally adaptable signal-in-space. This signal is the interface between the airport and the user aircraft. It allows the variety of airport MLS service configurations to operate with any aircraft of any MLS capability. Since the signal-in-space is generated by the airport, there will be a hierarchy of signals, progressing from that of minimum approach services (Cat. I) to the more sophisticated landing services (Cat. II and III). The most important aspect in the design of the signal-in-space is that there be a single signal structure, from which functions may be omitted by airports of lesser MLS capability, or which are not used by aircraft of lesser MLS capability. It is vital that a high capability aircraft not be confused in flying into a low capability airport and that a low capability aircraft be able to cope with a full MLS signal format.

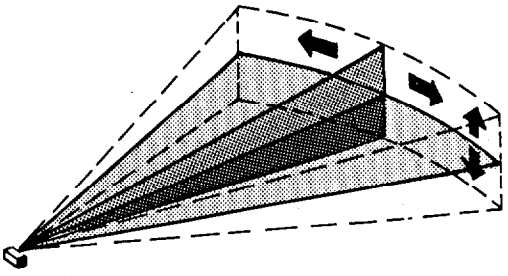

Fig. 2—Scanning Beam for Angle Data (No Modulation).

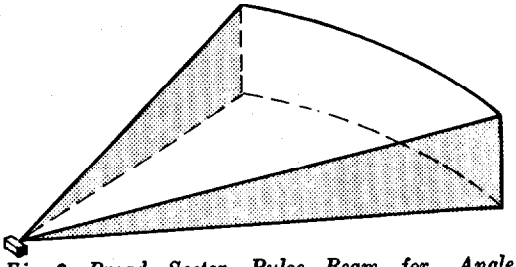

Fig. 3—Broad Sector Pulse Beam for Angle Function Identity and Other Landing Information Data (DPSK Modulation).

The signal format is based on time division multiplexing (TDM), wherein each angle guidance function is transmitted in sequence and all are transmitted on the same RF carrier frequency. The multiplexing of the various angle functions is termed the "scan format." The MLS scan format in conjunction with the detailed parameters of each time slot comprise the signal format (Fig. 4).

The scanning beams are scanned rapidly "to" and "fro" (back and forth for azimuth, down and up for elevation) at a precise rate. Each complete scan cycle results in two pulses—one in the "to" scan, the other in the "fro" scan. An aircraft receiver in the coverage volume derives its position angle directly from the measurement of the time difference between the "to" and "fro" scan pulses (Figure 5).

Decoding the signal format is simple—it is based on the notion of a clock. The "to" scan turns the clock "on," and the "fro" scan turns the clock "off." The angle measurement is accomplished by: (Fig. 5)

(a) Starting the angle counter on the leading edge of the "to" dwell gate at half the normal clock frequency (F_0).

(b) Transitioning to full clock frequency on the trailing edge of the "to" dwell gate.

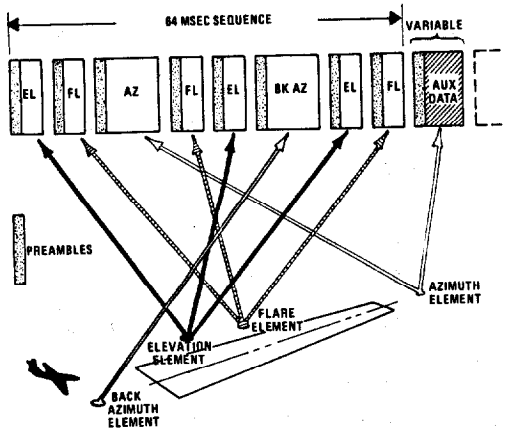

Fig. 4—Time-Multiplexed Function Signal Format.

(c) Reverting back to half clock frequency on the leading edge of the "fro" scan.

(d) Stopping the counter on the trailing edge of the "fro" scan.

(e) The number in the counter now represents the time difference between the centroids of the dwell gates and is a direct indication of the guidance angle.

Important parameters which characterize the TRSB are the sampled data pulse width (beam envelope dwell time) and the rate of its occurrence (scan rate). They will be used below to derive the basic TRSB angle equation.

The MLS Distance Measuring Equipment (DME) provides range information to each suitably equipped aircraft making an approach and landing at an airport. Several levels of DME accuracy are available to provide ICAO Cat. I approach service, through precise, fully automatic, Cat. III landing and rollout guidance.

Some functions performed by the DME are:

- Decision Height Marking—Forms MLS altimeter when used with approach elevation angle guidance. Replaces marker beacon and the radar altimeter.
- Complements the radar altimeter flare maneuver for runways with difficult front course terrain by blending from MLS altimeter to radar altimeter.
- Forms flare altimeter in conjunction with the flare guidance element.
- Desensitizing angle guidance, i.e., conversion of angle information to linear displacement information.

The capability to move the ground antenna

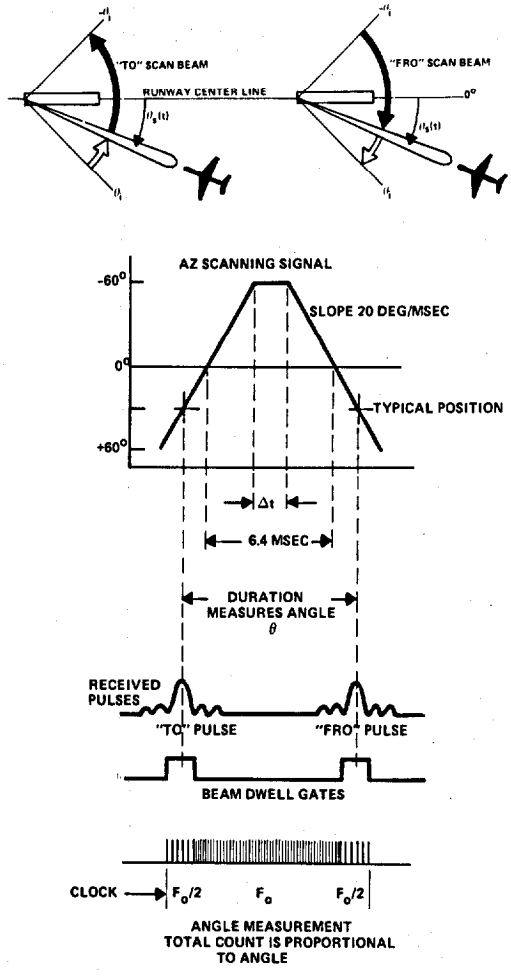

Fig. 5.—Principle of Angle Measurement.

fan beams at a constant angular velocity in either direction is the key to the time reference concept. The technique is based on electronically scanned antennas (E-Scan) whose beam steering commands can accurately control the position of the fan shaped beams in space as a known function of time. The high scan rate capabilities of E-Scan antennas allows:

- Cyclic and random guidance error perturbations induced by multipath to be reduced to operationally insignificant levels by aircraft "motion averaging."*
- Control motion noise introduced by multipath to be maintained at low levels consistent with good pilot acceptance factors such as the Cooper 2 ratings.

* The "motion averaging" concept will be discussed in detail later.

Table 1

GUIDANCE FUNCTION	AZIMUTH	ELEVATION	DME
LATERAL COVERAGE	±40°	80°	80°
VERTICAL COVERAGE	0 TO 20°	1 TO 20°	0 TO 20°
DATA RATE	13.5 Hz	40 Hz	40 Hz
ANTENNA BEAMWIDTH	1°	1°	–

The TRSB has been designed for implementation in three major configurations; (1) Basic, (2) Expanded, and (3) Small Community. The basic configuration is designed to provide Cat. I and II service, employing different antenna arrays to meet particular runway and environmental needs. The expanded configuration is designed with full redundancy to satisfy all Cat. III requirements. The small community configuration is intended for short runways at airports requiring a minimum level of approach and landing service. Additional configurations have been defined to satisfy military requirements.

The TRSB concept has the advantage of total modularity and interchangeability of the various ground elements. The system concept allows a range of antenna types and accuracies to be available, and the user can select the most economical mix of components for any required configuration and still be assured of complete interoperability between different installations.

Airborne designs also stress the modularity concept so that all users may independently procure only what they consider essential, while still obtaining service from all ground facilities. To obtain approach and landing guidance at the lowest cost at any TRSB equipped airport, an aircraft need have only an antenna, and a receiver-processor unit operating with existing flight instruments. At the other extreme, an aircraft equipped for Cat. III will carry redundant equipment and failure warning systems normally associated with such operations. Aircraft equipment is designed to be modular, so that an aircraft can be upgraded in the future without obsoleting its existing MLS equipment.

The signal format shown in Fig. 4 applies to the full format which would be employed at an airport having all the MLS guidance elements. This paper will address the "Basic Wide" facility

in which only the primary azimuth, approach elevation and DME guidance elements are used.† The system will have Cat. III accuracy guidance functions but will not meet the Cat. III redundancy and monitoring requirements. Table 1 summarizes the system. The data rate is not constant but has a slight jitter which ensures that the system will be insensitive to the effects of propeller modulation and multipath with high fluctuation rates. The jitter is induced by varying the duration of the auxiliary data time slot (Figure 4) in a random manner after the transmission of each 64-microsecond sequence of angle guidance functions.

An example of the "basic wide" implementation is shown in Fig. 6. The azimuth and elevation elements shown are line phased arrays. They are one of the many antenna hardware implementations available to the TRSB.

The TRSB Angle Code and Error Equations

A basic premise of the TRSB is that the guidance data should be coded directly in angle. Therefore the ground antenna beam steering commands should be programmed such that the TRSB scanning beam $\theta_s(t)$ sweeps at a constant rate. Given this premise, the defining angle-coded scanning beam equation is

$$d\theta_s(t)/dt = -2/K \tag{1}$$

where K is a constant. Integration of (1) with respect to time yields

$$\theta_s(t) = -\frac{2t}{K} + \theta_i \tag{2}$$

where θ_i is the initial scan start angle. Refer to Figure 5 for the definition of $\theta_s(t)$. Let t_R be the time between the "to" and "fro" scans—then Eq. (2) can be rewritten in terms of t_R and t_0 (the time separation in microseconds for 0°). The beam position time, t, is determined by subtracting $t_R/2$ from the full "to" scan plus half the scan pause time, Δt. That is

$$t = 2\left(\frac{K}{2}\theta_1\right) + \frac{\Delta t}{2} - \frac{t_R}{2} \tag{3}$$

Inserting (3) into (2) yields the fundamental TRSB equation

† Basic systems installed on long runways (13,000 ft.) are called "Basic Wide" and short runway installations (8000 ft.) are called "Basic Narrow."

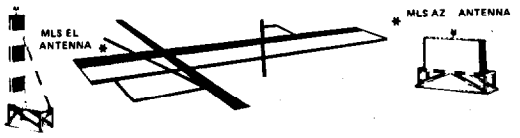

Fig. 6.—Basic MLS Ground System.

$$\theta_s(t) = \frac{t_R - t_0}{K} \tag{4}$$

where $t_0 = K\,\theta_i + \Delta t$

For azimuth t_0 = 6.8 msec and t_0 = 0.4 msec for elevation. The angle code scaling factor K = 100 microseconds/degree. Letting τ equal the time necessary for the antenna to scan one beamwidth, BW, allows K to be expressed in terms of the beam envelope dwell time and the antenna 3 dB beamwidth (i.e., $1/K = BW/2\tau$). The fundamental TRSB error equation can be obtained by taking the differential of (4) obtaining

$$\delta\theta_s = (BW/2\tau)\delta t_R \tag{5}$$

Previous discussions have shown that the angle measurement is a time determination t_R between the centroids of the "to" and "fro" scanning beams. A perturbation which displaces the beam envelope centroid from the true beam pointing angle will result in an error. Fig. 7 defines the measurement where

$$t_c = (t_L + t_T)/2 \tag{6}$$

Any disturbance of the leading or trailing edge beam envelope threshold crossing (δt_L or δt_T) such that there is a net perturbation δt_c will result in a beam pointing error for a "to" or "fro" scan. Typically, multipath will effect one or the other of the threshold crossings.‡ Therefore a leading or trailing edge perturbation δt will cause a centroid displacement $\delta t_c = \delta t/2$. Furthermore, band limited perturbations (less than 500 Hertz) will distort the "to" and the "fro" scans in an identical manner.§ For this case $\delta t_R = 2\delta T_c$ as illustrated in Fig. 8. The TRSB error equation becomes

$$\delta\theta_s = (BW/\tau)\delta t_c \tag{7}$$

An immediate consequence of (7) is that only the symmetry of one of the scans need be investi-

‡ In the present context antenna sidelobe patterns are considered second order disturbances.

§ Corresponds to elevation guidance element with 'to'-'fro' scans separated by 1 msec or more.

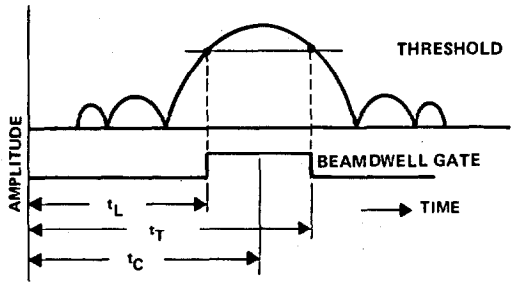

Fig. 7.—Centroid Measurement.

gated. The beam dwell time τ has been chosen to be 50 μsec for the azimuth and elevation guidance elements.

TRSB Accuracy Definitions

To properly understand the effects of multipath on the angle measurement, MLS accuracy definitions and their operational implications must be reviewed.‖

The accuracy specifications discussed below are referenced to the minimum guidance altitude (MGA) of the configuration under discussion. The allowed degradations away from the MGA in both the horizontal and vertical dimensions of the service coverage are specified in the MLS Functional Requirement Specifications (FRS), see Ref. 1.

Beam bias is overall misalignment of a specific course. This includes the MLS ground system as well as the MLS airborne receiver bias which cannot be reduced to zero by amplitude or delay adjustments in the receiver.

Beam noise is defined as spatial, temporal and resolution perturbations in the guidance signal. Beam noise and its effect on the safe landing of an aircraft can be best understood by viewing the beam noise in terms of its spectral density. In these terms the beam bias would be the lower frequency limit of beam noise. The beam noise samples arising from the receiver and ground transmitter are normally uncorrelated while for multipath the intersamples can be highly correlated. Thus their effects will have to be treated accordingly.

‖ The importance of the aircraft landing phase and landing guidance accuracy is highly evident in the statistics presented in Ref. 2, where it states that 55% of commercial jet accidents occur during the landing phase which is only 14% of the total flight exposure.

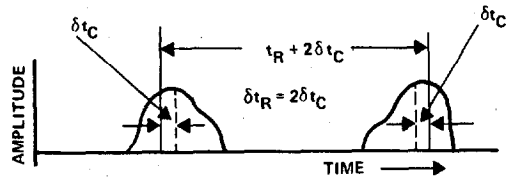

Fig. 8.—Beam Perturbation Errors.

To understand the effects of guidance perturbations on the MLS signal-in-space, the frequency response of the flight control system and the aircraft dynamics must be taken into account. The frequency response of the aircrafts lateral or vertical/longitudinal channel can be divided into three major spectral regions—a low, middle, and high frequency region. The low frequency region contains noise fluctuations which the closed loop guidance response of the aircraft can follow. That is the aircraft is physically displaced by these fluctuations. The middle frequencies result in control surface activity whose motions are too rapid for the aircraft to follow. The middle frequencies also include induced wheel (lateral channel) and column motion (longitudinal channel). Control response motion can lead to component wear-out and fatigue whereas column and wheel motion affect the pilot acceptance factors. The high frequency responses do not affect the aircraft guidance system or pilot and passenger comfort measures.

Three parameters describe the MLS accuracy measurement:

1) *Bias*—Overall course misalignment
2) *Path Following Noise*—Fluctuations which fall in the aircraft loop guidance bandwidth (similar to the ILS beam bends).
   Azimuth—0 to 0.5 radian/second
   Elevation—0 to 1 radian/second
3) *Control Motion Noise*—Fluctuations which induce control surface, wheel and column motion.
   Azimuth—0.3 to 10 radians/second
   Elevation—0.5 to 10 radians/second

The MLS Basic Wide accuracy specifications are listed in Table 2. It is generaly desirable to filter the raw MLS receiver output data samples to remove unwanted high frequency components before providing the data to the aircraft flight control system (AFCS). The filter should not only attenuate the unwanted components, but it must

not introduce excessive phase lag between flight path perturbations and indicated MLS output deviations. To meet these filter characteristics, the U.S. Government and industry AFCS designers have jointly established that a 10 radian/second single-pole filter will remove unwanted high frequency components, but it will not compromise the performance of AFCS (Ref. 1). The filtering can be performed at the output of the MLS receiver or it can be implemented where necessary in the FCS.

Multipath (General)

Although the multipath control theme presented in this paper is directed at the ground radiation elements of the Basic Wide configuration, it is typical of those applied in TRSB. The elements are the azimuth and elevation scanning beam functions, the broad sector preamble antenna, and the broad sector DME antenna. The azimuth and elevation radiation patterns are characterized by a scan pattern (narrow beam) and the non-scan pattern which is perpendicular to the direction of scan. The broad sector antennas have vertical patterns identical to the azimuth vertical pattern and lateral patterns which are similar to the elevation antenna lateral pattern.

The following sections will address multipath control as it applies both to the angular guidance beams and the broad sector coverage beams. The paper will also include a brief discussion of how the TRSB eliminates out-of-coverage false courses.

In-Beam and Out-of-Beam Multipath

Multipath interference can be categorized as either out-of-beam or in-beam. For out-of-beam multipath (Fig. 9), the direct and reflected signals are separated by at least 1.7 beamwidths so that they are received separated in time. In-beam multipath covers the case when the separation is less than 1.7 beamwidths and are received almost simultaneously.

Table 2

	AZIMUTH		ELEVATION	
BIAS	10 Ft.	0.044°	1.2 Ft.	0.06
PATH FOLLOWING NOISE**	9 Ft.	0.04°	1.4 Ft.	0.07°
CONTROL MOTION NOISE**		0.04°		0.05°

* ALL ERRORS ARE 2 SIGMA VALUES
**MAJOR PORTION OF BUDGET ALLOTTED TO MULTIPATH; MULTIPATH-FREE AIRBORNE AND GROUND EQUIPMENT ERRORS ARE NEGLIGIBLE.

AZIMUTH ERROR BASED UPON A 13,000-FOOT ANTENNA SITE TO MGA DISTANCE.
ELEVATION BASED UPON 1145-FOOT ANTENNA SITE TO MGS DISTANCE.

Criteria for the classification of multipath are shown in Figs. 15 and 16. Out-of-beam multipath is operationally minimized by the use of time gates in the receiver. The purpose of the time gate is to reject all signals except those arriving at the proper time.¶

In-beam multipath is a problem to all landing systems. It is caused by direct and reflected signals merging to form one distorted signal at the receiver; in *no* system can the two signals be easily separated. It is important then to minimize the possibility of in-beam multipath by using narrow beamwidths, low side lobes and the careful choice of radiation coverage (including tailored coverage) for each installation.

In-beam multipath effects arise because of the basic interference phenomena associated with the amplitude and phase characteristics of electromagnetic waves. A direct signal and a reflected signal from the same source will, when superimposed, create an interference field whose spatial dimensions depend upon the multipath geometry and the dimensions of the reflecting object. The amplitude, duration and frequency of the perturbations are most important. For example, the multipath frequency will determine whether the associated guidance perturbation is within the aircraft frequency response while the magnitude and duration of the disturbance may influence the probability of a safe landing. Only multipath effects arising from specular reflection will be treated since it is the predominate reflection mechanism.

Magnitude of Multipath Errors

This section demonstrates how the magnitude of the multipath induced errors can be calculated. First a useful approximation is derived followed by a discussion of the reflection coefficient. Finally curves are presented which give the exact magnitudes of the multipath induced errors.

a) Approximation to Maximum Error

The fundamental TRSB multipath error source mechanism is a perturbation which affects the

¶ The airborne receiver signal acquisition and validation functions will not be discussed in this paper.

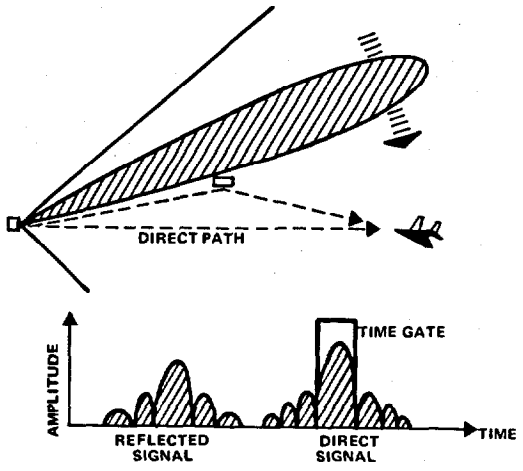

Fig. 9—Out-of-Beam Multipath.

symmetry of the scanning beam envelope about the threshold crossing points. Its effect can be quantified by an approximation which is useful in MLS scanning beam analysis work.

The approximation is derived as follows. Let e_D and δe_R be the peak direct signal amplitude and peak reflected signal respectively as shown in Fig. 10. Then for small disturbing signals, δe_R, the centroid of the beam will be displaced an amount

$$\delta t_c = \frac{1}{2\dfrac{de_D}{dt}} \delta e_R \tag{8}$$

From Fig. 11 the derivative at the −3 dB threshold crossing for a "Taylor weighted" beam positioned at boresight is

$$\left.\frac{de_D}{dt}\right|_{-3dB} = \frac{e_D}{T_{RT}} \cong \frac{e_D}{\tau} \tag{9}$$

Letting $\rho = \delta e_R/e_D$ equation (8) becomes $\delta t_c = \rho\tau/2$ which after inserting into (7) yields the approximation promised above.**

$$\delta\theta_S = \tfrac{1}{2}\rho BW \tag{10}$$

The ratio of the undesired signal to the desired signal is a function of:

- Indirect signal source amplitude, e.g., main beam, side lobe or the non-scan dimension of the antenna pattern.

** Log video receivers are used in TRSB. The results are unaffected by the linear receiver assumption.

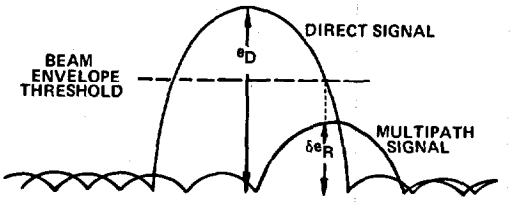

Fig. 10—In-Beam Multipath.

- The free space differential path delay.
- The specular reflection coefficient of the scattering surface.

b) Magnitude of the Reflection Coefficient

The specular reflection coefficient requires additional comment. It is specular in the sense that the reflected radiation conforms to the geometric optical law of reflection. The coefficient is a function of reflector size, surface roughness, surface contour and polarization. The radiation intensity reflected from a surface in the specular direction is proportional to the square of the projected specular area of the surface, if the transmit and receive antennas are in the far field of the surface. For MLS the reflector is typically in the far field of the ground antenna but the receiver antenna is usually in the near field of the reflector. In the near field, the surface acts like an infinite ground plane and reflects all the incident radiation. When the reflection geometry is such that all of the incident power is reflected in the specular direction the antennas are said to be in the Fresnel zone of the reflecting surface. For such a configuration any increase in size of the reflecting surface will cause ripples in the reflection pattern but will not provide any basic increase in reflection power gain. The minimum surface area which produces this effect is referred to as the first Fresnel zone or the "footprint size" of the surface. The Fresnel zone is an ellipse whose dimensions are dependent on the distances and orientation of the reflecting surface with respect to the ground and airborne antennas. Appendix A gives the approximate equations which define the Fresnel zone. Fig. 12 illustrates the vertical multipath specular reflection geometry for the Bendix azimuth test site at NAFEC in New Jersey.

Surface roughness tends to diffuse the reflected energy and therefore lower the specular reflection coefficient. Similarly, the reflector surface contour can modify the magnitude of the reflected radi-

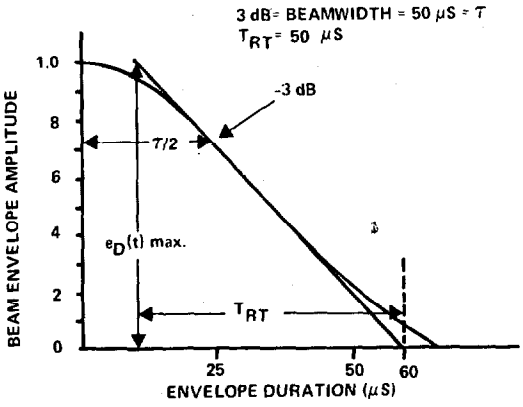

Fig. 11.—Taylor-weighted Beam Envelope.

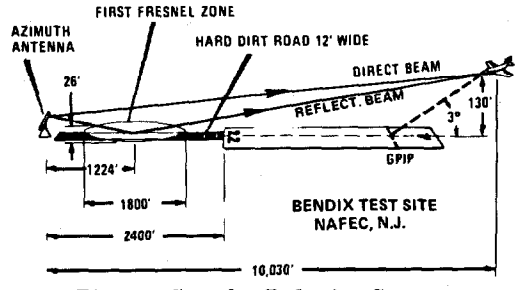

Fig. 12—Specular Reflection Geometry

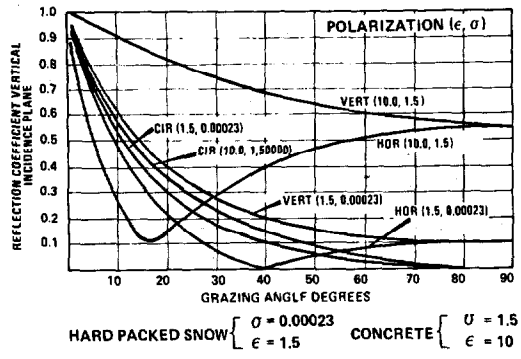
POLARIZATION (ε, σ)
REFLECTION COEFFICIENT VERTICAL INCIDENCE PLANE
VERT (10.0, 1.5)
CIR (1.5, 0.00023)
CIR (10.0, 1.50000)
HOR (10.0, 1.5)
VERT (1.5, 0.00023)
HOR (1.5, 0.00023)
GRAZING ANGLE DEGREES
HARD PACKED SNOW σ = 0.00023 ε = 1.5
CONCRETE σ = 1.5 ε = 10

Fig. 13.—Typical Runway Reflection Coefficients.

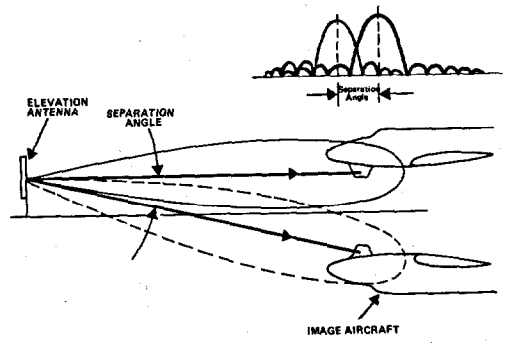

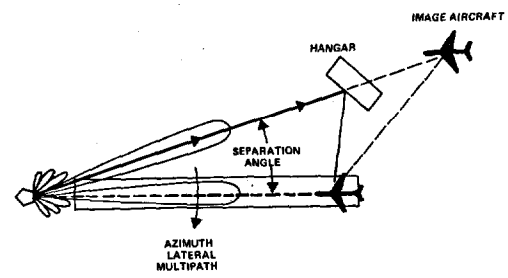

Fig. 14—Definition of Separation Angle.

ation whenever the reflector departs from a plane. Clearly the multipath problem is readily analyzed when the reflector corresponds to a flat plate.

From Fig. 13 it is evident that the reflection coefficient is a strong function of polarization. The TRSB transmitted polarization is vertical. However, relative to vertical reflectors it is horizontal. Fig. 13 gives the magnitude of the reflection coefficient for concrete and hard-packed snow vertical reflectors with respect to vertical, horizontal and circular polarized transmissions. Reverse the VERT and HOR labels for horizontal reflectors.

(c) *The Exact Multipath Error Calculation*

An exact multipath interaction formulation must account for the separation angle of the direct and reflected signals at the aircraft, ground antenna side lobes and the RF differential path delay. Fig. 14 defines the separation angle (SA).

The exact error magnitude in degrees per beamwidth is given in Fig. 15 for a Taylor-weighted far field pattern with −25 dB side lobes. The curves are for 180° RF phase. Note that $\rho BW/2$ acts as an upper bound on the in-beam errors at least for $\rho \leq -2$ dB. A similar family of curves is shown in Fig. 16 for 0° RF phase.

The undistorted antenna pattern is plotted in Fig. 17a. Fig. 17b graphically illustrates the combined direct and multipath signals for specular reflections 6 dB below the desired beam. The multipath separation angle is half a beamwidth and the curve is plotted for an RF differential phase of 180°. Note the shift of the beam centroid. A 0° RF phase case is shown in Fig. 17c for a 1.7

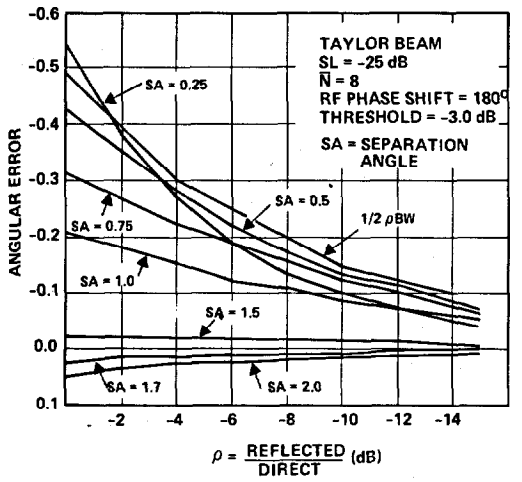

Fig. 15.—Multipath Errors (180° RF Phase Shift).

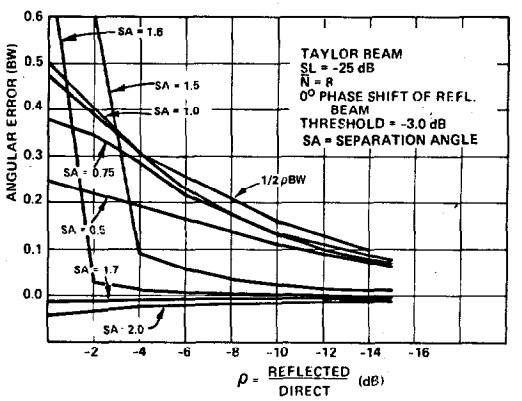

Fig. 16.—Multipath Errors (0° RF Phase Shift).

BW separation angle and a multipath level equal to the signal level. For this case both of the −3 dB direct signal points can be measured. As mentioned above and shown in Fig. 16 this case represents the dividing line between in-beam and out-of-beam multipath.

Multipath Induced Error Fluctuation Rate

Consider the elevation guidance element multipath interaction geometry shown in Fig. 18. The lateral in-beam multipath induced instantaneous error $\delta\theta_s$ is then a function of φ_{RF}, ρ, α, β, and γ. The variable φ_{RF} is the *RF* phase delay of the reflected wave relative to the direct wave. As the aircraft moves along its flight path (velocity V) variables for $\delta\theta_s$ will change as a function of time. In most cases the RF phase delay φ_{RF} fluctuates more rapidly than the other variables. Appendix B derives the rate of change of φ_{RF} for the case where the reflection point does not change position too rapidly. The result is

$$f_s = d\varphi_{RF}/dt = (V/\lambda)\ (\cos\alpha - \cos\beta) \quad (11)$$

Therefore the direct and indirect signals will vary in and out of phase at rate f_s with the effect that the composite beam envelope will also fluctuate, inducing a periodic error $\delta\theta_s(t)$. The duration of the cyclic error will depend upon the specular dimensions of the reflector and the reflection geometry. The spectrum of $\delta\theta_s(t)$ can be obtained using Fourier Analysis. The nearly discrete sinusoidal components (highly peaked portions of the spectrum) can be investigated for their effect on the aircraft FCS. Components which are below 10 radians/second may interact with the aircraft FCS. For high frequency components the error perturbation will be averaged to operationally insignificant levels by the 10 radians per second MLS receiver output filter and the aircraft guidance loop.

The periodic variation in $\delta\theta_s(t)$ is termed the scalloping frequency in the landing guidance system literature. Fig. 19 is a plot of f_s vs. distance from threshold for the geometry shown. Note that the scalloping rate is constant only over a small spatial region. It changes slowly at long range and rapidly as the aircraft approaches runway threshold. This will be treated in a later section.

Primary In-Beam Multipath Geometries

All the four multipath geometries shown in Fig. 18 and in Fig. 20 can be analyzed using Eq. (11), Figs. 15 and 16 and reflection coefficient curves similar to Fig. 13. The separation angle and the antenna radiation pattern angles can all be determined using geometric optic imaging theory. Fig. 18 and Fig. 20(b) are equivalent multipath situations; the lateral reflection obstacle in the elevation case is replaced by the ground in the azimuth vertical multipath configuration. Similar remarks apply to Figs. 20(a) and 20(c) which are also equivalent. Each case will be treated individually below, but basic multipath control techniques will be discussed first. The first is the technique of *radiation control.* There are two approaches: Coverage Control and Pattern Control. Coverage control is defined as a

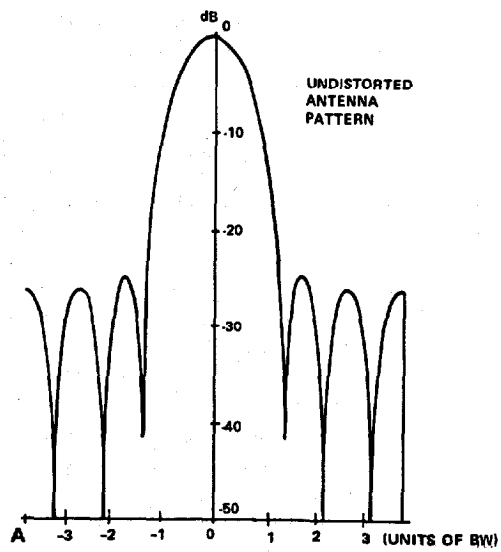

Fig. 17a.—Undistorted Beam.

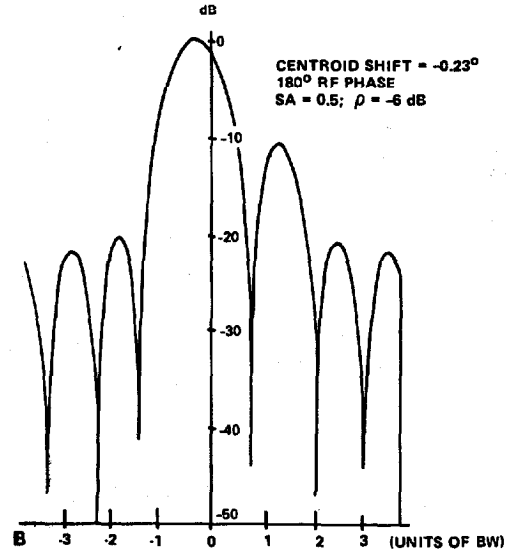

Fig. 17b.—Distorted Beam ($\rho = -6db$).

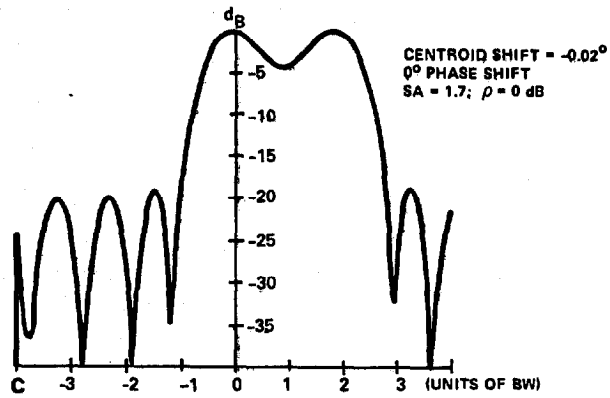

Fig. 17c.—Distorted Beam ($\rho = 0db$).

restriction of coverage in the guidance plane (i.e., in the direction of scan). Pattern control is defined as illumination control in the plane perpendicular to the guidance plane.

Low Angle Elevation Vertical Multipath (Fig. 20a)

Low elevation multipath reflections from the ground are controlled in TRSB by antennas designed to have narrow elevation beams, low side lobes and the application of coverage control. The principle is simply to provide low angle guidance while at the same time minimizing the illumination of the ground with the beam. It is important to minimize these reflections because they affect both the minimum height at which elevation guidance can be provided over the runway and the obstacle clearance plane criteria. The ground antenna beam widths are selected so as to avoid the ground and satisfy these criteria.

Multipath from the ground is characterized by a low scalloping frequency which can not be effectively filtered by the aircraft FCS. The minimum elevation guidance height over the runway can be determined using Fig. 16 and the separation angle geometry of Fig. 14. For example a 1 degree antenna will allow the aircraft to descend to a height corresponding to 1.7° separation angle. At a 1000 ft. distance, the minimum guidance height above the runway

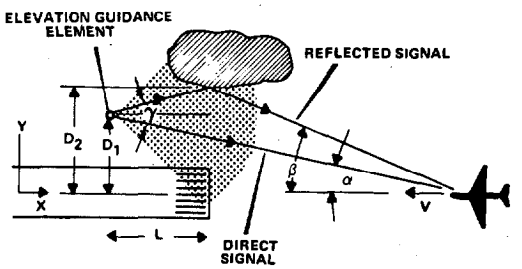

Fig. 18.—Lateral Elevation Multipath.

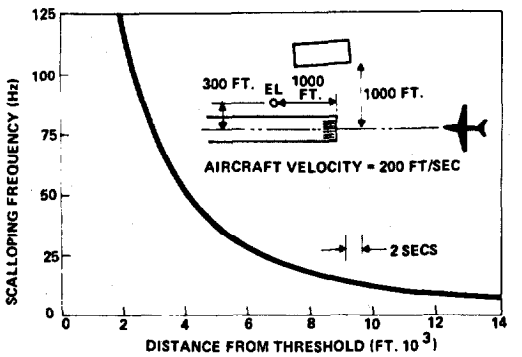

Fig. 19.—Scalloping Frequency vs. Distance.

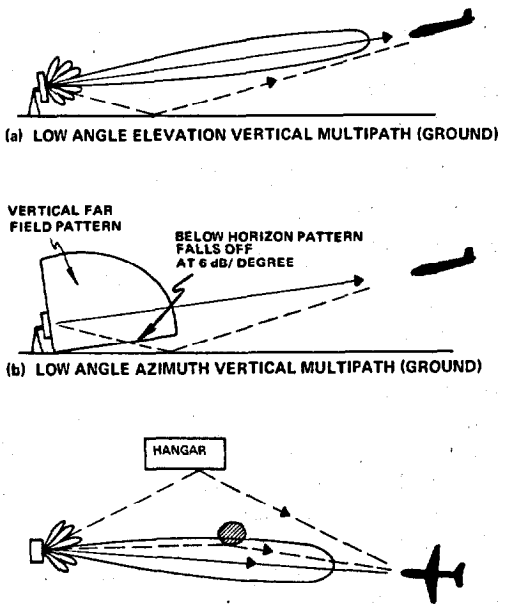
(a) LOW ANGLE ELEVATION VERTICAL MULTIPATH (GROUND)
VERTICAL FAR FIELD PATTERN
BELOW HORIZON PATTERN FALLS OFF AT 6 dB/ DEGREE
(b) LOW ANGLE AZIMUTH VERTICAL MULTIPATH (GROUND)
HANGAR
(c) AZIMUTH LATERAL MULTIPATH

Fig. 20.—In-Beam Multipath Geometries.

would be about 15 feet (or 30 feet for a 2° beam). The important point is that low-angle guidance below 50 feet permits auto-lands at runways which have irregular front course terrains where radar altimeter data may be highly inaccurate. The elevation guidance when combined with DME range forms an MLS "altimeter" which provides highly accurate aircraft height in the vicinity of runway threshold. When the aircraft is safely over the runway, the height calculations transition from the MLS "altimeter" to the radar altimeter.

As indicated above ground antenna beam widths are also selected to satisfy the obstacle clearance planes. Fig. 21 illustrates the separation angle geometry and presents the criteria definitions and specifications. See Ref. 3 for details. TRSB with its low angle guidance capabilities could allow these approach surface minimums to be lowered.

Even lower angle guidance can be obtained if elevation coverage control is applied using power programming techniques. In this technique the beam is scanned down to a fixed angle. The beam is held there for a given time period during which the transmitter power is attenuated in a

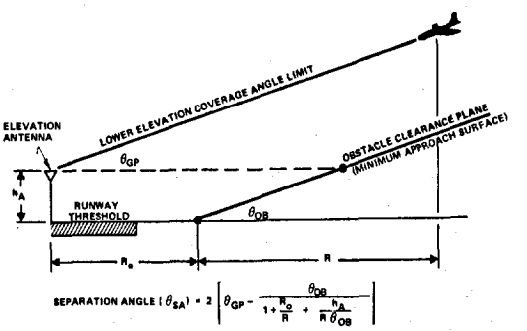

CAT II MINIMUM APPROACH SURFACES FOR R < 10,000 FT.		
θ_{GP}^*	θ_{OB}	SURFACE SLOPE
1.5°	0.6°	94:1
1.9°	1.1°	50:1
2.3°	1.7°	34:1

*θ_{GP} = 0.75 (GLIDE SLOPE)

Fig. 21—Obstacle Clearance Plane Criteria.

prescribed manner versus time. Thus the transmitter power is programmed so as to simulate the continued scanning of the beam and the ground is not illuminated below the fixed scan

angle. In conclusion, TRSB multipath control techniques can achieve accurate guidance at lower elevation minimums than have been established for ILS.

Low Angle Azimuth Vertical Multipath (Fig. 20b)

The TRSB azimuth sites are insensitive to ground terrain because they employ pattern control to the vertical antenna radiation pattern. This is accomplished through the use of a large vertical aperture. Large antenna vertical dimensions allow aperture illumination functions to be specified in such a manner that "far field" patterns are developed which fall off rapidly below the horizon (see Fig. 20b) and thus limit the energy which otherwise would be reflected from the ground. The aperture is large in terms of the C-band wavelength of 2″, but it is physically small—being only 4 feet when slotted waveguide column antennas are employed.

A typical radiation pattern including worst case ground reflection effects is shown in Fig. 22. The phase center height is 7.28 feet. This height is chosen as a compromise between low-angle coverage attenuation (below .33° in the figure) and the pattern "ripple" frequency. This trade-off is made evident by considering the reflection geometry also shown in the figure to be an interferometer. As shown in the figure full gain is available at glide paths greater than 2° and at long ranges. At the runway threshold 50 feet reference point, the elevation angle would be 0.35° for an 8000 feet runway and 0.19° for a 15,000 feet runway. The azimuth signal amplitude would only be attenuated 4 dB and 10 dB respectively which is far less than the signal increase resulting from the decreasing path loss. Finally the design shown in Fig. 22 will provide accurate signal guidance down through aircraft touch down and roll out. The depth of the pattern null is a measure of how much energy is reflected from the ground.

This section has shown that pattern control as applied to the azimuth antenna vertical pattern will allow an azimuth site design which is insensitive to the surrounding ground terrain.

Azimuth Lateral Multipath (Fig. 20c)

Azimuth ground elements produce fan beams, narrow in the horizontal plane, and are well protected from in-beam multipath. Obstacle clear-

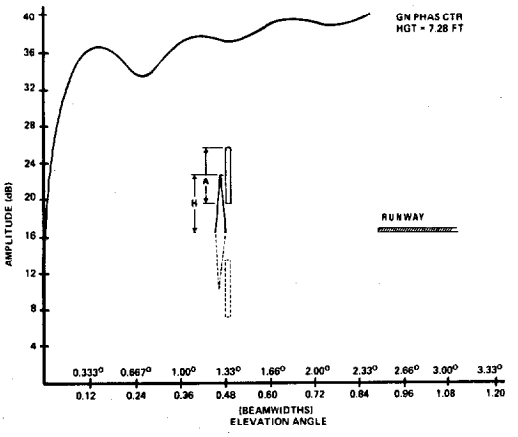

Fig. 22—Azimuth Antenna Vertical Pattern.

ance regulations keep the areas near runways clear of fixed objects and greatly minimize the possibility of azimuth in-beam multipath on final approach. Fig. 23 shows that even for 13,000′ runways all reflections originating outside the critical clearance zones produce out-of-beam multipath signals. A taxiing aircraft near threshold, may produce some in-beam multipath, however the errors are small. For the worst case orientation of the 747 tail plane the errors are less than 0.03° (Ref. 6). Coverage control can be applied to the azimuth site by limiting the sector coverage about runway centerline.

MLS accuracy standards are based upon linear errors in cartesian coordinates referenced to the MGA. Ground antenna accuracies are however, specified in terms of angular error and beamwidth. This means that the azimuth angular errors at the MGA are inversely proportional to runway length. A trade-off between beamwidth and runway length can be made using the fundamental relation $\rho BW/2$. In conclusion TRSB using narrow scanning beams and coverage control effectively suppresses azimuth lateral multipath.

Elevation Guidance Lateral Multipath (Fig. 18)

Elevation ground elements have a narrow-beam in the vertical plane, but a wide-beam in the azimuthal (or horizontal) plane; they are susceptible to in-beam reflections by buildings, etc., within the coverage zone of the system and for lower angle approaches. In particular, if structures have been built in the region opposite runway threshold under current ICAO obstacle

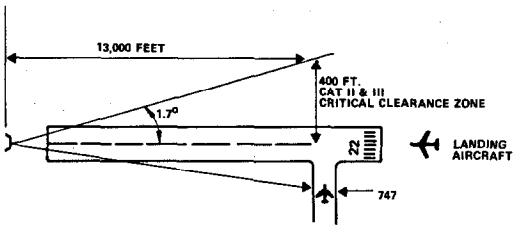

Fig. 23—Azimuth Lateral Multipath Geometry.

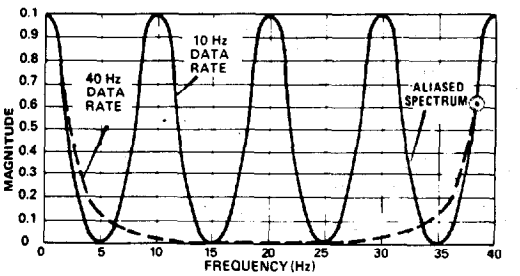

Fig. 24.—Digital Filter.

clearance regulations, they can be sufficiently high to cause in-beam reflections during final approach on glideslopes up to 3–4 degrees.

As noted previously, when the aircraft moves across the interference field generated by the direct signal and the signal reflected by an obstacle, the angle measurement error for each sample oscillates at the scalloping frequency. Depending upon the reflection geometry the scalloping frequencies can be very high; beyond 300 Hertz (Figure 19).

The TRSB high scan rates (sampled data rates) allow averaging of the sampled errors over an interval in proper relationship with the scalloping period and may substantially reduce it. This motion averaging is especially beneficial for the case of elevation lateral multipath, when the accuracies of individual sampled measurements are near the limits of the error budget. Combined with pattern control, motion averaging is an effective means of reducing lateral in-beam multipath.

The key point is the relationship between the scan rate and the scalloping period. Since the TRSB is a sampled data system, the sampling process itself must be accounted for in the system design. Unlike analogue systems, sampled data signal processing must contend with spectrum fold-over or aliasing. Even though the multipath scalloping frequency may exceed the aircraft FCS bandwidth (10 radians/second) the multipath perturbation may be aliased down into the FCS bandwidth. This will be the case whenever the disturbing frequency is equal to the scan rate or is a harmonic of this rate. More precisely, if the aircraft flight control system passband is Δf and the sampling frequency is f, then the aliasing will occur at $nf \pm \Delta f$ where n is an integer. That is, the sampling process causes higher frequencies to reappear in the low frequency passband. Clearly, high scan rates will yield better averaging performance. Fig. 24 is the frequency response of a digital 2-pole 10-radians-per-second BW Butterworth filter computed for scan rates of 10 Hertz and 40 Hertz.†† This filter or its equivalent is inserted at the output of the angle receiver. The frequency responses about the aliasing frequency are called "grating lobes."

The effects of scan rate on wideband uncorrelated noise can be easily discerned. Suppose the standard deviation for each sample at the 10-Hertz rate is σ then a 40-Hertz system with the same bandwidth will have a standard deviation of $\sigma/\sqrt{4}$ when averaged down to a 10-Hertz system.

The conclusion is obvious from Figure 24. The error-energy under the response curve of the 10-Hertz system is approximately four times the error-energy of the 40-Hertz system. The amplitude reduction (voltage) of the 40-Hertz system to the wide band noise then is the square root of 4.

In order to demonstrate the effectiveness of the TRSB format and implementation in dealing with in-beam multipath, a complete computer simulation of the system was undertaken. The simulation used the Bendix elevation antenna Taylor-weighted array pattern for the narrow portion of the scanning beam and employed a tapered pattern for the lateral or wide portion of the fan beam (-3 dB at $\pm 20°$). Fig. 25 shows the geometry of a representative airport siting situation for an aircraft having a 150 feet/second approach speed. Reflection coefficient for the

†† The Digital 2-Pole Butterworth filter has an 8-degree phase lag at one radian/second and as such may not be acceptable to all FCS designs. Five to six degrees of phase lag is considered as acceptable. The single pole filter described in Fig. 29 has an acceptable phase lag of 5.7 degrees.

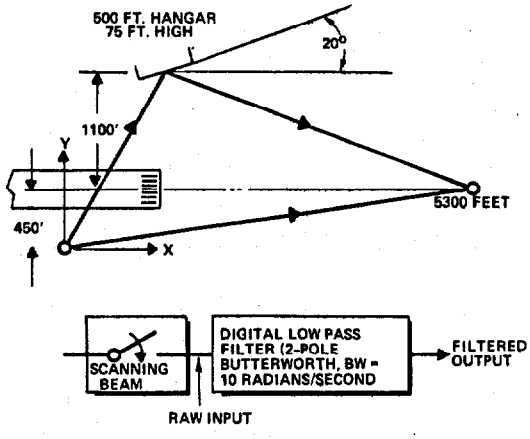

Fig. 25.—Lateral Multipath Geometry.

hangar is −3 dB. The processor block diagram (Fig. 25) uses the filter described above as the MLS angle receiver output filter.††

The multipath separation angle was calculated assuming the hangar was rotated 20 degrees from the x-axis. Fig. 26 displays the filter output for sampling frequencies of 5, 20 and 40 Hertz.

The multipath disturbance lasted for 18 seconds; it began at 4400 feet from threshold and ceased at around 1700 feet from threshold when the specular reflection point moved off the hangar. At 4400 feet (or zero seconds on the plots) the scalloping frequency was about 23 Hertz, at 10 seconds it was 40 Hertz, and at 15 seconds it was 60 Hertz. These times are confirmed graphically for the 20-Hertz data rate shown in Fig. 26, where the second (40-Hertz) and third (60-Hertz) aliased frequency ranges (grating lobes) are self evident. The first grating lobe is not shown because the lowest scalloping frequency is 23 Hertz. At the 40-Hertz data rate, only the first grating lobe is present because the high scalloping frequency is less than 68 Hertz. The multiscan error is no more than 0.02 degree except for a 1 to 2-second portion which never exceeds 0.05 degree.

The approximate duration for the aircraft to fly through a 40-Hertz sampling rate grating lobe can be determined as follows. The passband Δf is 10 radians/second (1.6 Hertz). The time duration for the scalloping frequencies to change from $f_s - \Delta f$ to $f_s + \Delta f$ is given by

$$\Delta t = 2 \cdot \Delta f \cdot 1/(df_s/dt) \qquad (12)$$

The reciprocal of df_s/dt is called the persistence

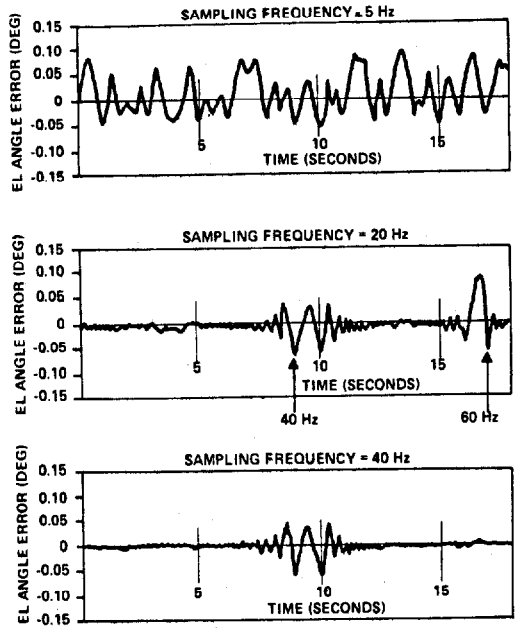

Fig. 26.—Fig. 25 Filtered Output.

in MLS literature. A plot of the persistence versus scalloping frequency is presented in Fig. 27. Using Eq. (12) and Fig. 27 the time for the aircraft to fly through the 40-Hertz grating lobe is about one second which corresponds to a 2-second filter response as shown in Fig. 26. It is important to note that passage times through the grating lobes decrease as the scalloping frequencies increase. Thus as the aircraft approaches runway threshold (the critical region) the perturbations are of short duration.

Figure 28 is another elevation multipath siting situation where the hangar is 75 feet high and 2500 feet long. Using Fig. 18; D_1 = 450 feet, D_2 = 1700 feet, and L = 900 feet. Aircraft speed was 200 feet/second. The hangar was chosen to be unusually long so that a wide range of multipath scalloping effects could be observed. Note the filter output is now but a series of transients. The analysis above was based upon a uniform scan rate. However as mentioned above each 64 msec scan sequence is varied in time relative to the previous scan sequence. These time variations have a random-like pattern which is repeated after the transmission of 8 sequences. The average transfer function for this jitter format is shown in Fig. 29 for an average sampling frequency of 40 Hz. The digital filter has a

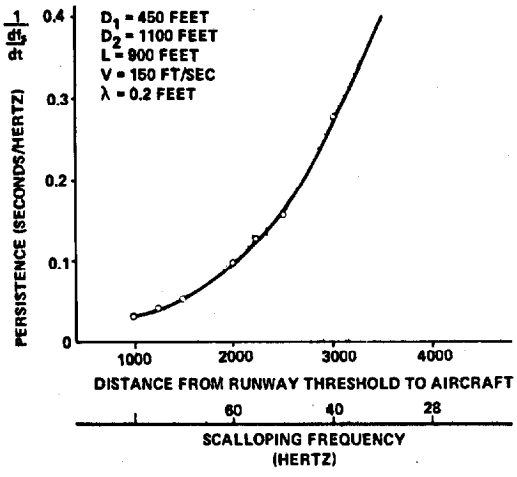

Fig. 27.—Persistence vs. Distance.

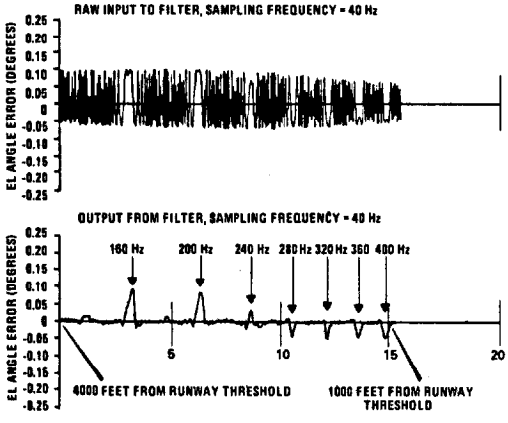

Fig. 28.—Long Reflector Lateral Multipath.

single pole and has been designed with a 10 rad/sec bandwidth. This filter has been implemented in the Bendix ICAO airborne receivers which are presently being used in flight tests at NAFEC, N.J. Notice in Fig. 29 that the aliased spectrum peaks have been reduced at least 6 dB. Examination of the sampling process, at harmonics of the sampling frequency, illustrates the randomness within each cycle of the samples obtained. Effectively, noise is produced over a broader spectrum than the filter bandwidth thereby reducing the power output. Thus the aliased error peaks shown in Figs. 25 and 28 can be reduced at least by a factor of two. Under this assumption the error perturbations are well within the path following and control motion noise error budgets listed in Table 2. Although the filter

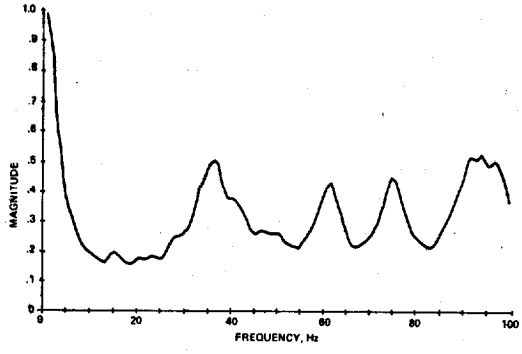

Fig. 29—Average Transfer Function (Single Pole Filter) for TRSB Jitter Format. Average Sampling Frequency = 40 Hz, BW = 10 rad/sec.

described here is different than the one used in the simulations their effects on the aliased spectrum peaks in the context of this discussion would be similar.

The above simulations demonstrate that the TRSB with lateral antenna pattern control will effectively suppress multiscan errors presented by representative airport geometries.

Multipath Effects on the Preamble Transmission

The function preamble transmission sources are located at each guidance element site. The DPSK modulation is applied directly to the carrier at a 15-kHz bit rate. Multipath affects the preamble DPSK modulation by reducing the signal-to-noise ratio which in turn increases the bit error rate. The TRSB has been designed with adequate signal power margin to minimize the signal fades. Also the broad sector antennas have been designed with both horizontal and vertical pattern control.

Out-of-Coverage False Course Suppression

The elimination of false courses outside of the service coverage is obtained by broad sector transmission in the out-of-coverage region. These transmissions establish thresholds in the airborne receiver which suppress the ground antenna back lobes.

Conclusion

A system has been described which will control multipath induced errors to acceptable limits by using high data rates, narrow scanning beams, radiation control and pattern control. These ideas will be tested at the Bendix test site runway 4/22 at NAFEC New Jersey during July 1976.

Acknowledgement

The author wishes to thank P. Wang and J. Gallant of Bendix Communications Division for their computer programs.

References

1. MLS Functional Requirement Specification. FAA-ER-700-07, February 1975.
2. Fries, J., "Commercial Aviation Benefits to be Derived from the MLS" DOT-FA72WA-3010, December 1974.
3. FAA Advisory Circular AC120-29, Dated 9/25/70.
4. Beckmann, P. and Spizzichino, A., "Scattering of Electromagnetic Waves from Rough Surfaces," Pergamon Press, 1963.
5. Evans, J. E., et al, "TRSB Critical Area Studies—Part I: Reflection Effects", Lincoln Lab ATC Paper 44 wp-5028, November 5, 1975.

Appendix A—Dimensions of the First Fresnel Zone

The size of the Fresnel zone can be approximated by (Ref. 4)

$$L = r\frac{\sqrt{\left(1+\frac{2\delta_0}{\lambda}\right)}}{1+\frac{(h_T+h_R)^2}{\lambda r}}$$

$$W = \sqrt{\lambda r}\sqrt{\frac{(1+2\delta_0/\lambda)}{1+\frac{(h_T+h_R)^2}{\lambda r}}}$$

$$\delta_0 = \frac{2h_T h_R}{r}$$

where

L = major axis of ellipse; length of first Fresnel zone along plane of incidence.
W = minor axis of ellipse; width of the first Fresnel zone.
h_T = height of ground antenna phase center.
h_R = height of airborne receiver antenna.
λ = RF wavelength.
r = ground distance between ground antenna and the airborne receiver.

Appendix B—The Multipath Interference Equations

Using Fig. 18 let

direct signal plane wave =

$$e^{i\varphi_D} = e^{i(\bar{K}_D\cdot\bar{r}_D-\omega_0 t)} \tag{1}$$

Reflected plane wave =

$$\rho e^{i\varphi_R} = \rho e^{i(\bar{K}_R\cdot\bar{r}_R-\omega_0 t-\theta_0)} \tag{2}$$

where

$$\bar{K}_D = (2\pi/\lambda)\bar{\epsilon}_D \tag{3}$$
$$\bar{K}_R = (2\pi/\lambda)\bar{\epsilon}_R \tag{4}$$
$$\overline{dr}_D/dt = -V\cos\alpha\bar{\epsilon}_D \tag{5}$$
$$\overline{dr}_R/dt = -V\cos\beta\bar{\epsilon}_r \tag{6}$$
$$d\varphi_D/dt = -(2\pi/\lambda)V\cos\alpha - \omega_c \tag{7}$$
$$d\varphi_R/dt = -(2\pi/\lambda)V\cos\beta - \omega_c \tag{8}$$

Deviations do not include the assumed constant path delay from the antenna to the reflector. The carrier frequency and wavelength are ω_c and λ respectively. Unit vectors along the propagation direction of the plane waves are $\bar{\epsilon}_D$ and $\bar{\epsilon}_R$ with $\bar{r}_D$ and $\bar{r}_R$ the respective position vectors. θ_0 is the phase of the reflection coefficient. The ratio of the reflected signal to the direct signal is ρ and V is the aircraft velocity. At the airborne receiver the direct and reflected signals combine to form

$$\text{Resultant} = e^{i\varphi_D} + \rho e^{i\varphi_R} = A(t)e^{i\varphi(t)} \tag{9}$$

where

$$A(t) = \sqrt{1+\rho^2+2\rho\cos(\varphi_R-\varphi_D)} \tag{10}$$

$$\varphi(t) = -\omega_c(t) + \Delta\varphi + \bar{K}_D\cdot\bar{r}_D \tag{11}$$

and

$$\Delta\varphi = \tan^{-1}\left[\frac{\rho\sin(\varphi_R-\varphi_D)}{1+\rho\cos(\varphi_R-\varphi_D)}\right] \tag{12}$$

The scalloping frequency f_s is

$$f_s = \frac{1}{2\pi}\frac{d}{dt}(\varphi_R-\varphi_D) = \frac{1}{2\pi}\frac{d\varphi_{RF}}{dt} \tag{13}$$

Using (7) and (8) Eq. (13) becomes

$$f_s = \frac{1}{2\pi}\left[\frac{d\varphi_D}{dt}-\frac{d\varphi_R}{dt}\right] = \frac{V}{\lambda}(\cos\alpha-\cos\beta) \tag{14}$$

When $\rho \ll 1$, Eq. (10) can be rewritten using (14) to obtain

$$A(t) \cong 1 + \rho\cos(2\pi f_s t) \tag{15}$$

That is the envelope of the multipath disturbance is a sinusoidal variation. In most applications f_s is a function of time as the aircraft moves through the interference field (Fig. 19).